

# Estimations of CO and NO<sub>2</sub> emissions and the fire combustion efficiency for fire activities over CONUS using TROPospheric Monitoring Instrument (TROPOMI) measurements

**Wei-Ting Hung<sup>1,2,\*</sup>, Barry Baker<sup>1</sup>, Patrick Campbell<sup>1,2</sup>, Youhua Tang<sup>1,2</sup>,  
and Gill-Ran Jeong<sup>1,2</sup>**

<sup>1</sup>Air Resources Laboratory, National Oceanic and Atmospheric Administration, MD, USA

<sup>2</sup>Center for Spatial Information Science and Systems, George Mason University, VA, USA

\*Correspondence: [whung@gmu.edu](mailto:whung@gmu.edu)

- **Abstract:**

This study quantifies the carbon monoxide (CO) and nitrogen dioxide (NO<sub>2</sub>) emissions ( $E_{CO}$  and  $E_{NO_2}$ ) from fire activities over the contiguous United States (CONUS) in 2020 using the total-column CO and NO<sub>2</sub> measurements from the TROPospheric Monitoring Instrument (TROPOMI) satellite. The contributions of local emissions, atmospheric transport, chemical loss, and averaging kernel are considered. The emission ratio ( $ER = E_{NO_2} / E_{CO}$ ) is used as a proxy of fire combustion efficiency. Preliminary results show that, TROPOMI  $E_{CO}$  shows a similar seasonal variation to fire emission inventories with significant enhancements during summertime while TROPOMI  $E_{NO_2}$  shows an opposite trend. TROPOMI ER also shows a significant seasonal variation, introducing the capability of attributing fire seasons associated with different fire and land types.

- **Keywords:** Fire emission; Combustion efficiency; TROPOMI

# Outline

- **Introduction**
  - Fire activities in the US
  - Fire emission estimation
  - Fire combustion efficiency
- **Objective**
- **Methodology**
  - Datasets
  - TROPOMI emission/ER estimation
- **Results and discussions**
  - Comparison between TROPOMI and emission inventories
  - Seasonal variation of TROPOMI ER
  - ER's capability of distinguishing fire and land types
  - Sources of uncertainties
- **Conclusions**
- **References**
- **Acknowledgements**

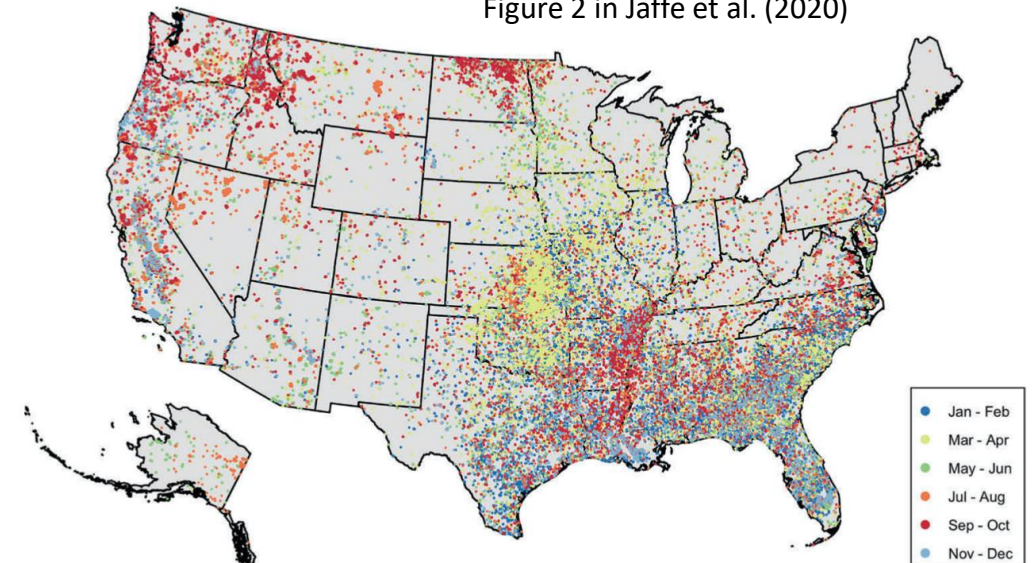
# Fire activities in the US

- Fire activities, including wildfires and prescribed fires, are important sources of trace gases and aerosols in the US.

Fire type	Season	Region	Fuel type
Wildfire	Summer and Fall	Western US	Forest
Prescribed fire (e.g. agricultural and deforestation fires)	Winter (Spring)	Southern (Central) US	Savanna and rangeland

- Prescribed fires are commonly used for land management. They are better managed under **specific meteorological conditions** (e.g.  $T < 80^{\circ}\text{F}/27^{\circ}\text{C}$  and  $\text{RH} = 40 - 60\%$  depending on regions) and are less intense compared to wildfires.

Figure 2 in Jaffe et al. (2020)



# Fire emission estimation

- Current emission inventories calculate fire emissions ( $E$ ) as the products of **total burned fuel loadings** ( $M_{\text{burned}}$ ) and **compound-specific emission factors** ( $F$ ).

$$E = M_{\text{burned}} \times F$$

- **“Bottom-up” approach:** estimate  $M_{\text{burned}}$  based on burned area ( $A$ ), total fuel loading ( $M_{\text{total}}$ ), and fraction of consumed fuel loading ( $FB$ )

$$E = (A \times M_{\text{total}} \times FB) \times F$$

- **“Top-down” approach:** estimate  $M_{\text{burned}}$  using satellite fire radiative energy ( $FRE$ ) and a prescribed combustion rate ( $\alpha$ )

$$E = \left( \alpha \times \int FRE \right) \times F$$

- Uncertainties of estimation of burned loadings and assumptions of compound-specific factors lead to **various results from different emission inventories.**

# Fire combustion efficiency

- Fire combustion efficiency is often used to describe **fire characteristics** (e.g. flaming or smoldering combustion).

- **Modified combustion efficiency (MCE)**, the most common fire combustion efficiency, is defined as CO<sub>2</sub> fire emission divided by total carbon emission (Yokelson et al. 1996). However, it is **hard to calculate MCE using satellite retrievals** with limited CO<sub>2</sub> measurements.

$$MCE = \frac{E_{CO_2}}{E_{CO} + E_{CO_2}}$$

- **Emission ratio (ER)** is defined as the ratio of NO<sub>2</sub> to CO fire emission, which is applicable for satellite retrievals.

- Recently, several studies used the **CO and NO<sub>2</sub> total-column measurements from TROPOMI** to estimate ER from space (Lama et al. 2020; Van der Velde et al. 2021), showing that ER is able to identify the spatiotemporal variabilities of fire characteristics.

$$MR = \frac{E_{NO_2}}{E_{CO}}$$

# Objective

- This study uses the total-column CO and NO<sub>2</sub> measurements from TROPOMI to quantify the daily CO and NO<sub>2</sub> fire emissions ( $E_{\text{CO}}$  and  $E_{\text{NO}_2}$ ) and emission ratio ( $ER = E_{\text{NO}_2} / E_{\text{CO}}$ ) over CONUS in 2020.
- Results are compared with five fire emission inventories:
  1. Preliminary 2020 National Emissions Inventory (NEI) from the United States Environmental Protection Agency (US EPA)
  2. Blended Global Biomass Burning Emissions Product (GBBEPx)
  3. Fire INventory from NCAR (FINN)
  4. Global Fire Assimilation System (GFAS)
  5. Quick Fire Emissions Dataset (QFED)

# Datasets

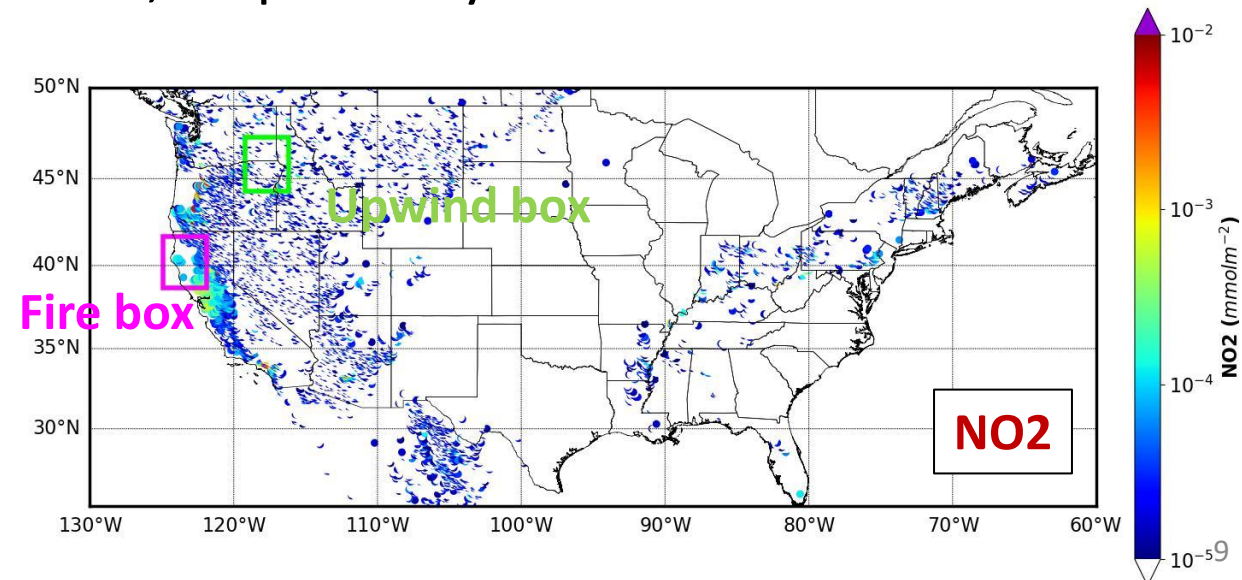
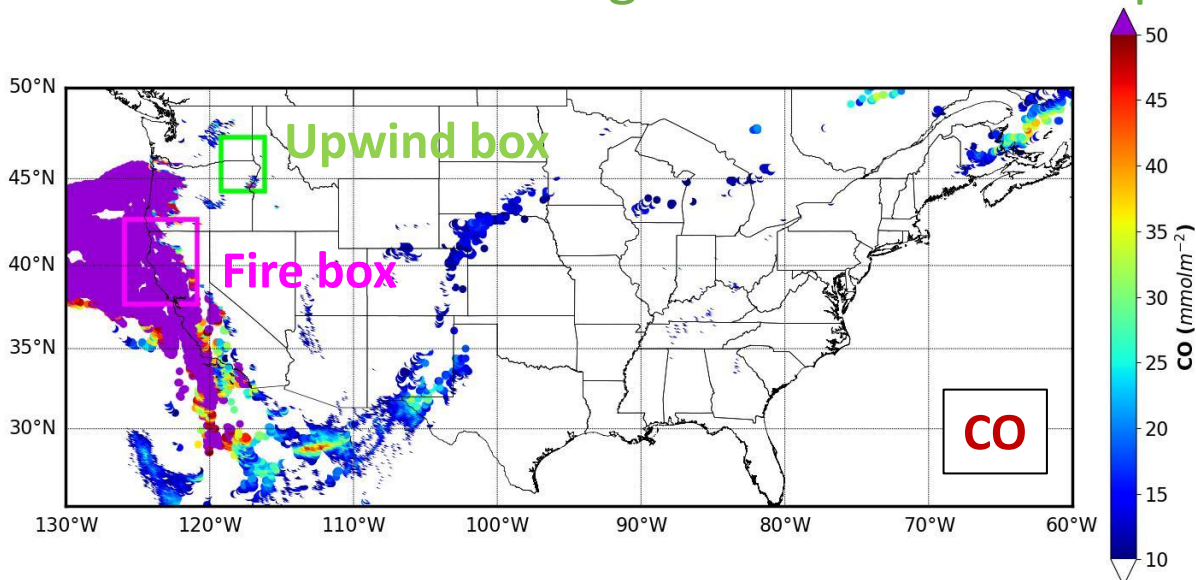
Dataset	Version/Level	Variable	Spatial Resolution
TROPOMI	V2/L2	Total-column CO density	5.5 km x 7 km
		Total-column NO <sub>2</sub> density	5.5 km x 3.5 km
EPA NEI	Preliminary	CO emission, NO <sub>x</sub> emission, Fire location, Fire description	
GBBEPx	V3.1	CO emission, NO <sub>x</sub> emission, Fire radiative power	0.1 degree
FINN	V2.5	CO emission, NO <sub>2</sub> emission	0.1 degree
GFAS	V1.2	CO emission, NO <sub>x</sub> emission	0.1 degree
QFED	V2.5/L3	CO emission, NO emission	0.1 degree
HRRR	V3	Horizontal winds (U, V)	3 km

- Year 2020, CONUS
- Data selection:
  - CO quality flag > 0.7, NO<sub>2</sub> quality flag > 0.75 (clear sky & thin cloud)
  - Measurements over snow- and ice-covered surfaces are removed.
  - Only fire points with FRP exceeding 95 percentiles (~65MW) are analyzed.
- Inventory NO<sub>x</sub>/NO emissions, except for FINN, are converted into NO<sub>2</sub> emissions by using a ratio of NO:NO<sub>2</sub> of 85:15 (Lobert and Warnatz, 1993).



# TROPOMI emission/ER estimation

- The annual medians of CO and NO<sub>2</sub> measurements on no-fire days are subtracted from total column measurements to **remove the influence of local sources other than fires**.
- For CO, a 5 x 5 degree fire box with fire point as the center and a 3 x 3 degree upwind box are selected. The upwind area is determined based on skirt distance (5 + 3 degree) and column-average winds within 7000 m from HRRR.
- Since NO<sub>2</sub> has relatively short lifetime (3 – 10 h) and is less affected by atmospheric transport, a 3 x 3 degree fire box is used while the size of upwind box and skirt distance are the same as CO.
- For each fire point, fire-affected ( $X_{\text{fire}}$ ) and background ( $X_{\text{background}}$ ) column densities are defined as the **averages of fire box and upwind box**, respectively.



# TROPOMI emission/ER estimation

- The influences of atmospheric transport and chemical loss are considered:

$$E_i = \Delta X_i \times \frac{U}{L} \times K_i [OH] [mol\ cm^2\ s^{-1}]$$

$$\Delta X_i = X_{i,fire} - X_{i,background}$$

$$K_{CO} = 1.1 \times 10^{-12} \times \left(\frac{T}{300}\right)^{1.3} [cm^3\ mol^{-1}\ s^{-1}]$$

$$K_{NO_2} = 2.8 \times 10^{-11} [cm^3\ mol^{-1}\ s^{-1}]$$

U: column-average wind within 7000 m ( $ms^{-1}$ )

L: diameter of fire center, 0.1 degree  $\sim$  11 km

K: OH reaction rate (Burkholder et al., 2015)

[OH]: average OH concentration within the PBL,  $1.5 \times 10^7$  mole  $cm^{-3}$  (Lama et al. 2020)

T: column-average temperature within 7000 m (K)

- To compare with fire emission inventories, TROPOMI ER is corrected by taking satellite averaging kernel ( $A_{influence}$ ) into account:

$$ER = \frac{E_{NO_2}}{E_{CO}} \frac{1}{(1 - A_{influence})}$$

$A_{influence}$ : 9% (Lama et al. 2020)

# Contributions of each factors

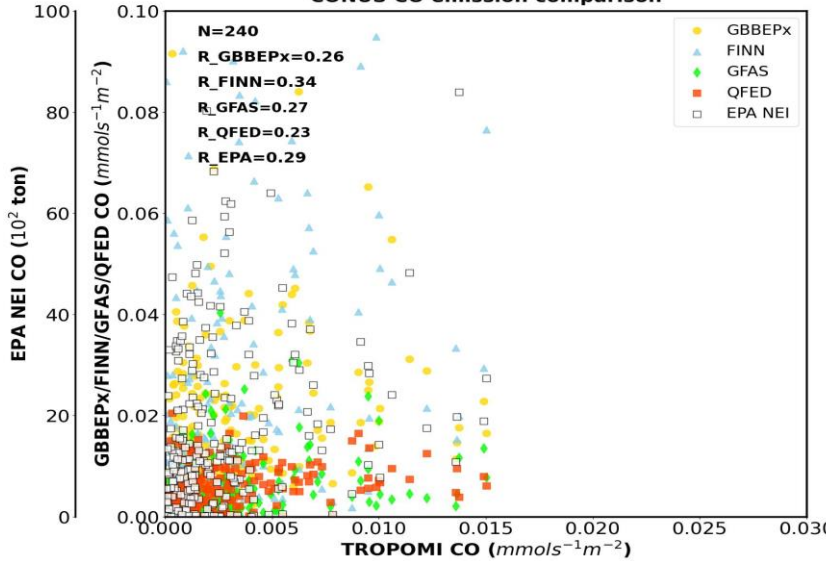
- Contribution for a specific term is determined by calculating the relative error between the fully-corrected results ( $X_{\text{corrected}}$ ) and results not considering this term ( $X$ ).
- Contribution =  $100\% * (X - X_{\text{corrected}}) / X_{\text{corrected}}$

(Unit: %)	Local emission	Transport	Chemical loss	Averaging kernel
CO	74.87	-96.03	-3.97	-
NO2	347.85	-55.29	-44.71	-
ER	496.01	1386.51	-45.72	-9

# TROPOMI – Inventory comparison

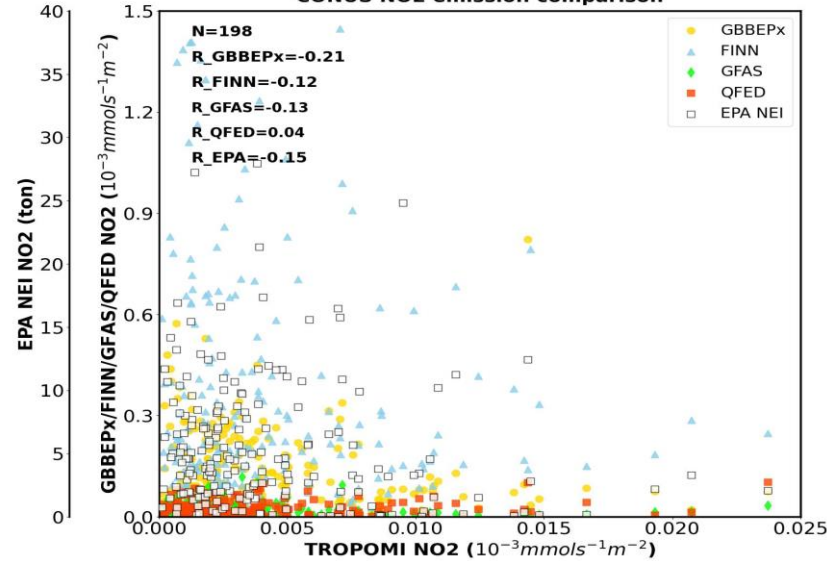
CO

CONUS CO emission comparison



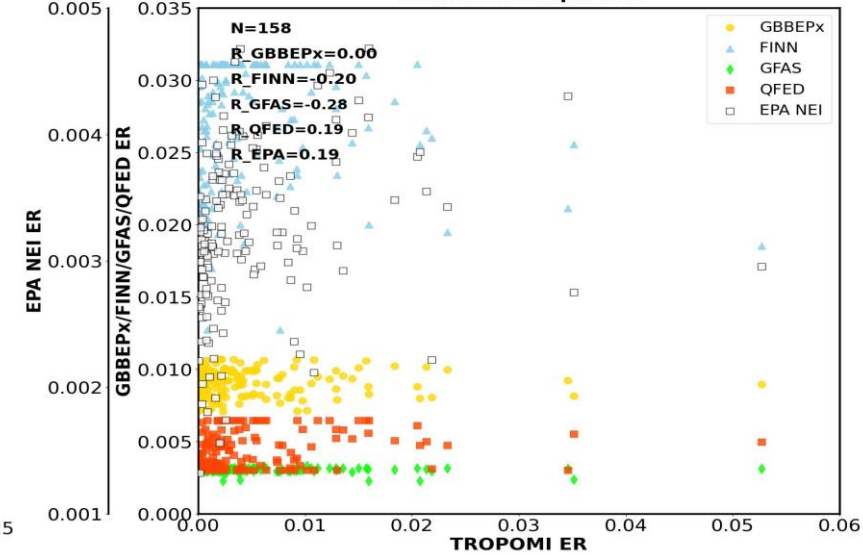
NO<sub>2</sub>

CONUS NO<sub>2</sub> emission comparison



ER

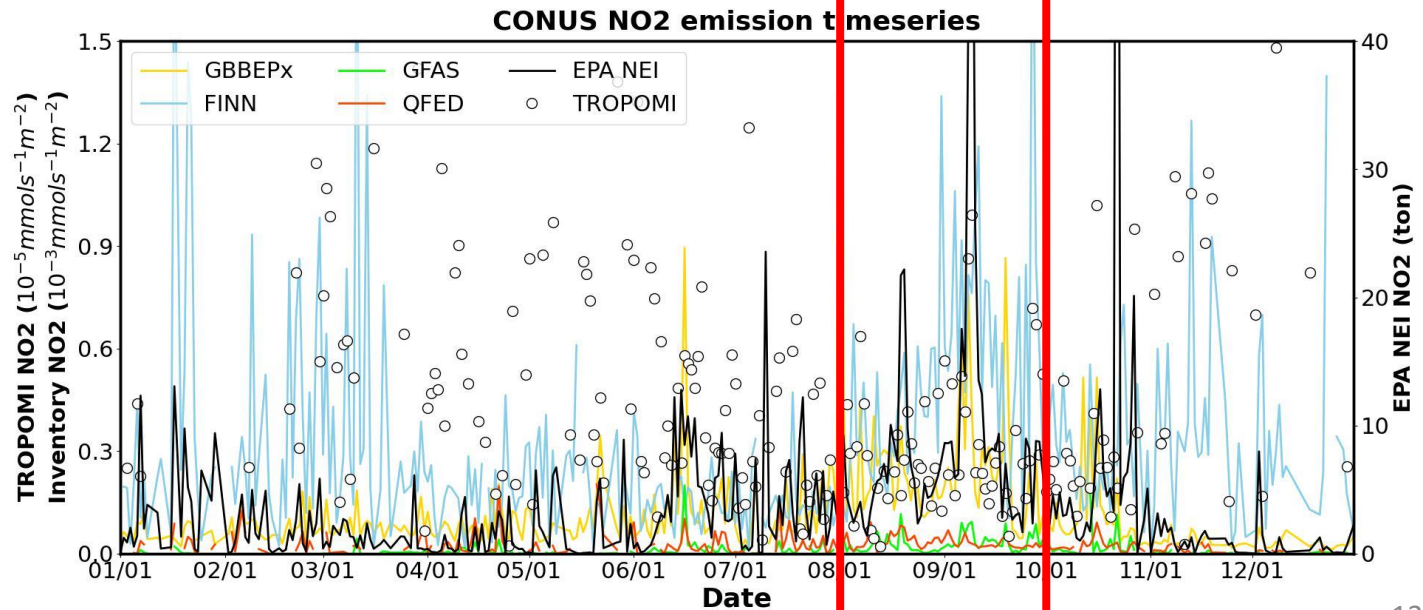
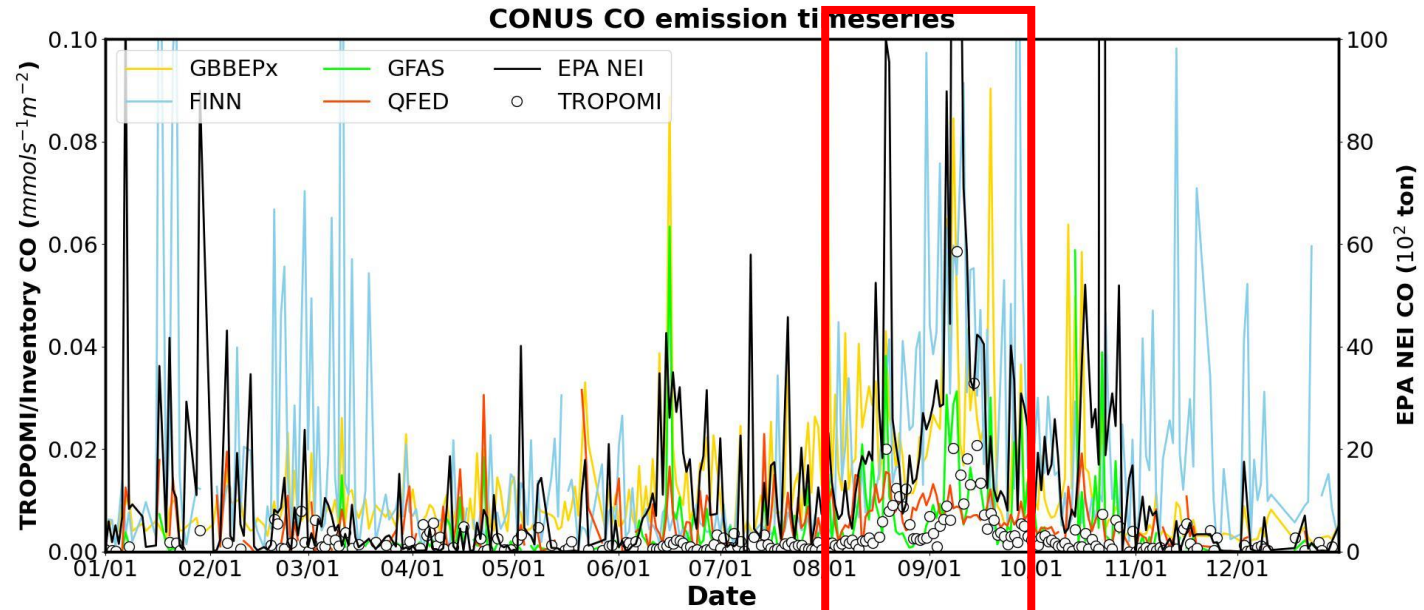
CONUS ER comparison



- Daily regional averages are calculated according to US EPA regional offices.
- Overall, TROPOMI emissions are much **lower than emission inventories**, except for EPA NEI.
- TROPOMI  $E_{\text{CO}}$  has moderate linear correlations with emission inventories with correlation coefficients ( $R_s$ ) around 0.3, while  $E_{\text{NO}_2}$  shows negative correlations and even no correlations.
- TROPOMI ER has larger variation compared to inventories, which have ER values fall in certain ranges probably due to the **prescribed emission factors** used in emission estimation.

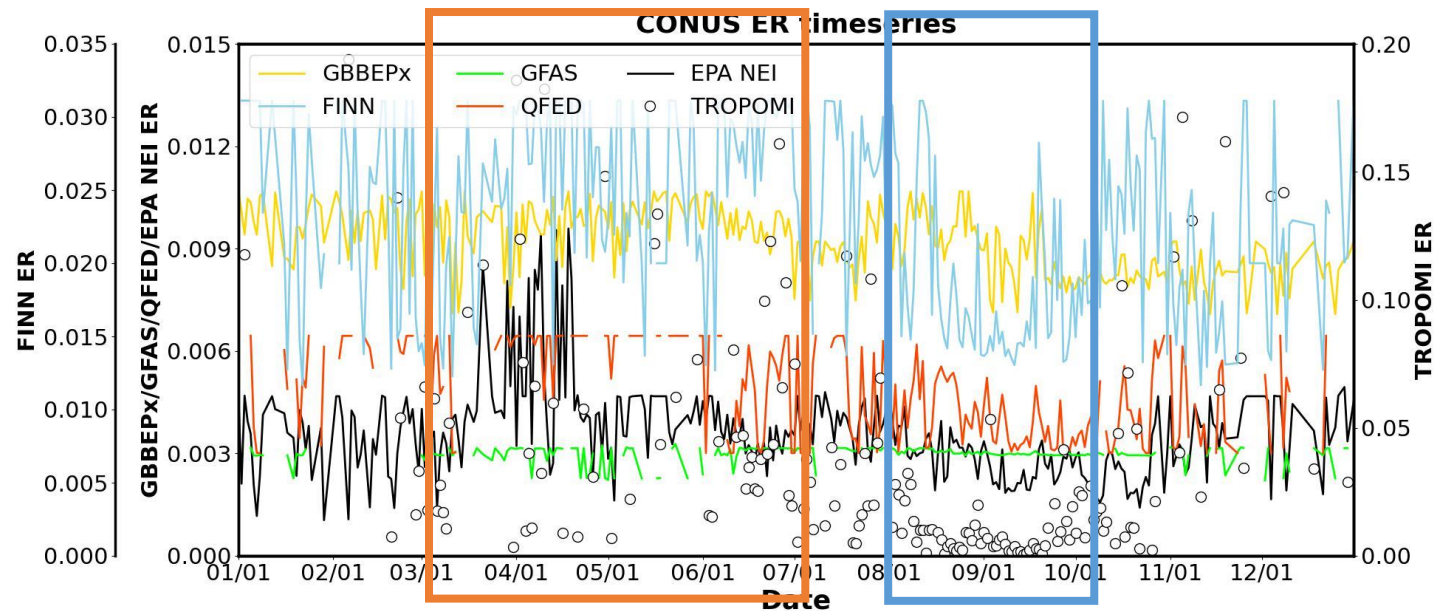
# TROPOMI – Inventory comparison: $E_{CO}$ , $E_{NO2}$

- TROPOMI  $E_{CO}$  shows significant seasonal variation with **increases during Aug – Sep (summer)**, corresponding to emission inventories.
- TROPOMI  $E_{NO2}$  is **lower during Aug – Sep (summer)**, showing an opposite trend compared to  $E_{CO}$  and emission inventories.



# TROPOMI – Inventory comparison: ER

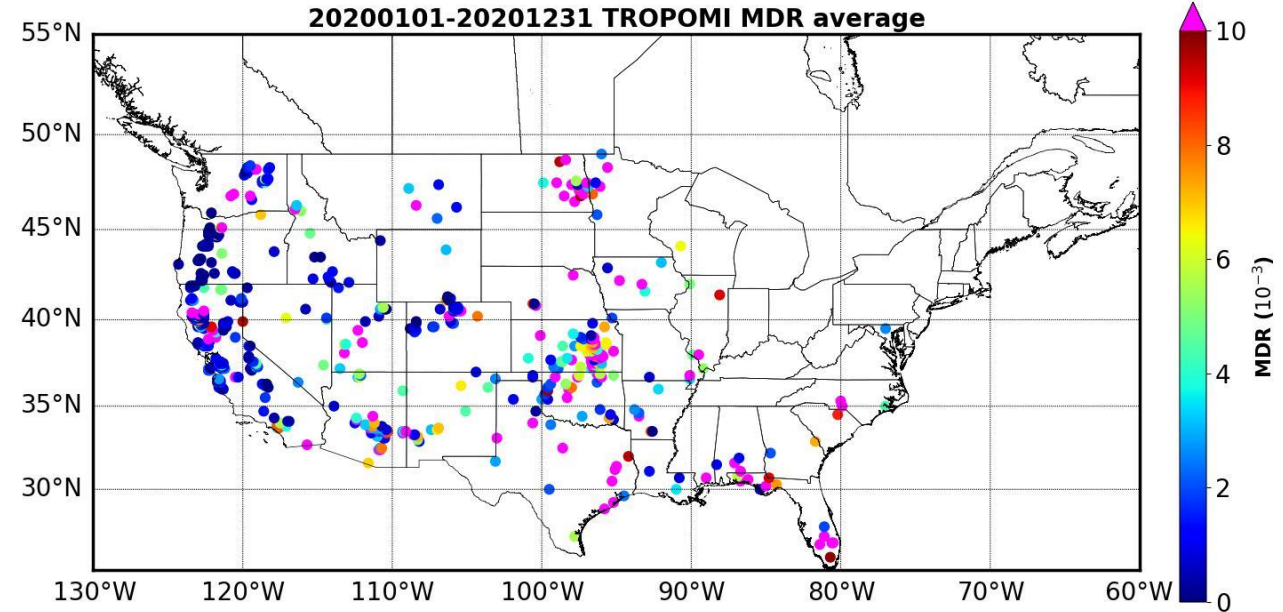
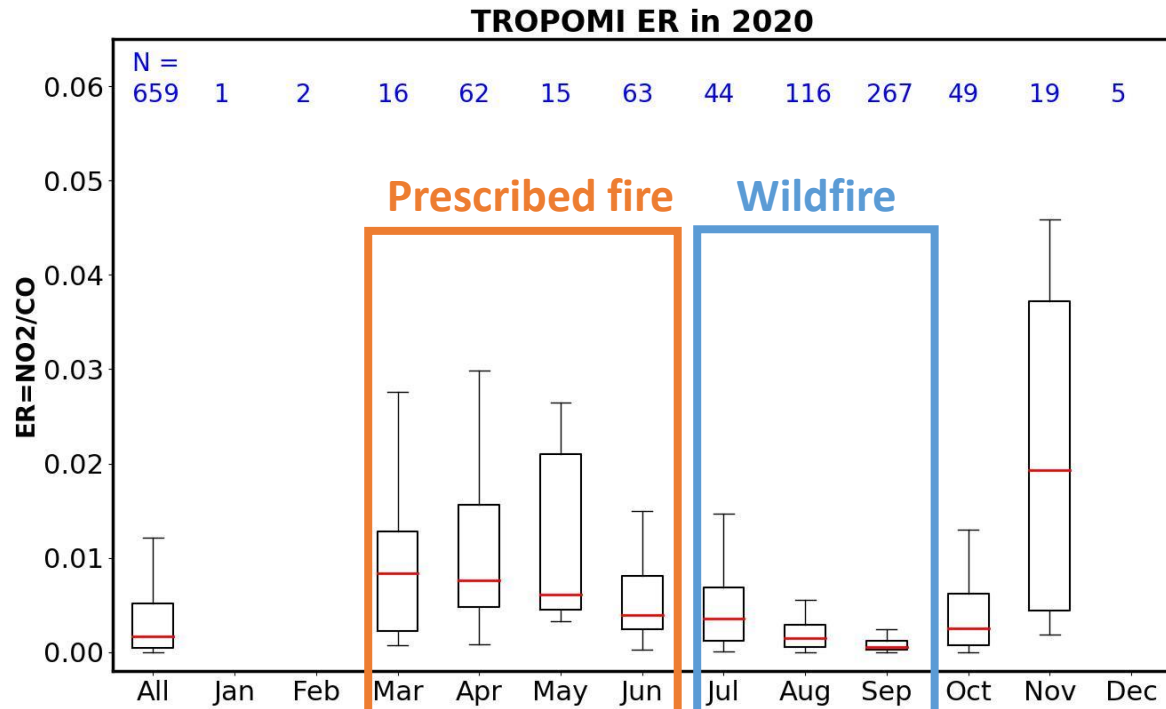
- GBBEPx and GFAS ERs are relatively consistent compared to TROPOMI and other inventories.
- TROPOMI ER is higher during **March – June** and significantly lower in **August and September**.
- TROPOMI, FINN, QFED and EPA NEI share a similar seasonal variation with the lowest ER in summertime, showing **the capability of distinguishing different fire seasons**.



# Seasonal variation of TROPOMI ER

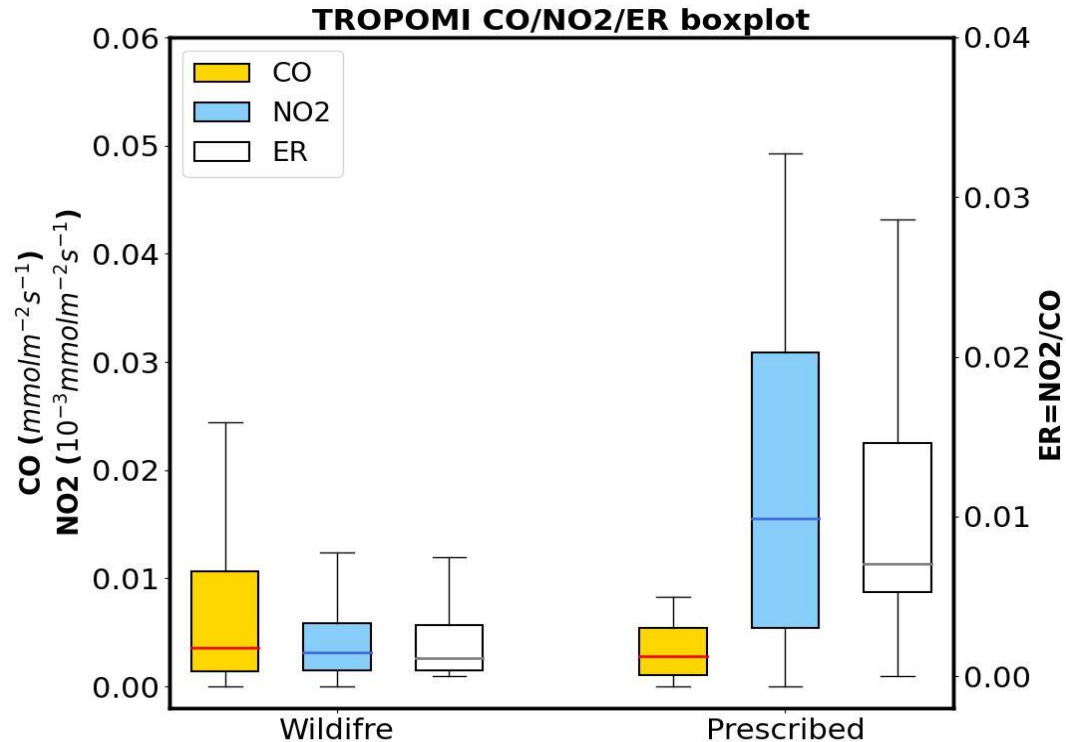
Months with less than 10 fire points are ignored.

Animation of monthly plots is shown in ppt.



- TROPOMI ER shows a clear seasonal variation with higher values in **spring (prescribed fire season in the central US)** and lower values in **summer (wildfire season in the western US)**.
- Because most of fire activities happen in summer and wildfires are relatively easily detected by satellites compared to prescribed fires, the annual ER is relatively low after averaging.
- Most of the high ERs occur over the central US while the low MDRs mainly occur over the western states, corresponding to different fire types.

# ER's capability of distinguishing fire types



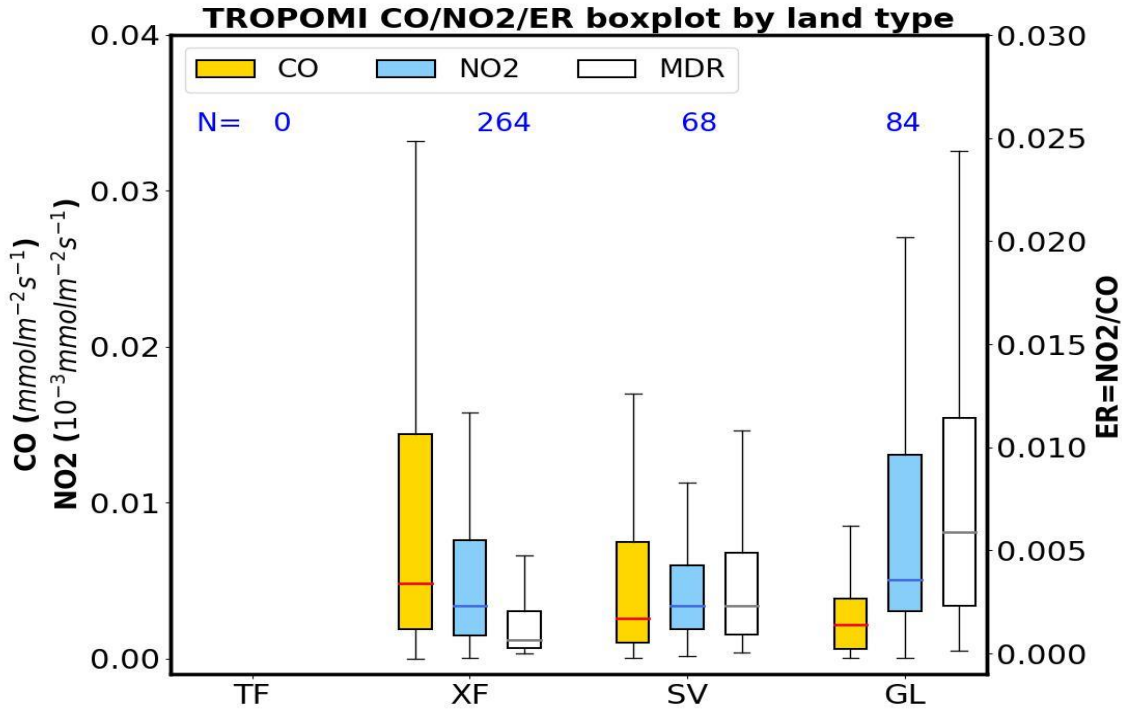
- Fire types are identified based on EPA NEI.
- TROPOMI ER is **lower for wildfire** and **higher for prescribed fires**, as  $E_{\text{CO}}$  ( $E_{\text{NO}_2}$ ) is higher (lower) for wildfires and lower (higher) for prescribed fires.
- Although the average  $E_{\text{CO}}$  for wildfire is higher than prescribed fire, the medians for two fire types are comparable, indicating a similar base condition of two fire types and the contribution of **extreme wildfire events**.
- The high  $E_{\text{NO}_2}$  for prescribed fire may be due to the **larger fraction of smoldering combustions** compared to wildfire, as  $\text{NO}_2$  contributes around 40% and 14% of total  $\text{NO}_x$  emissions in smoldering and flaming combustions, respectively (Lobert and Warnatz, 1993).

	Wildfire	Prescribed fire
$E_{\text{CO}}$ ( $\text{mmol m}^{-2} \text{s}^{-1}$ )	0.009±0.015 (0.004)	0.003±0.003 (0.003)
$E_{\text{NO}_2}$ ( $10^{-3} \text{mmol m}^{-2} \text{s}^{-1}$ )	0.004±0.004 (0.003)	0.018±0.013 (0.016)
ER	0.003±0.008 (0.001)	0.017±0.048 (0.007)

Value: avg±std (med)



# ER's capability of distinguishing land types



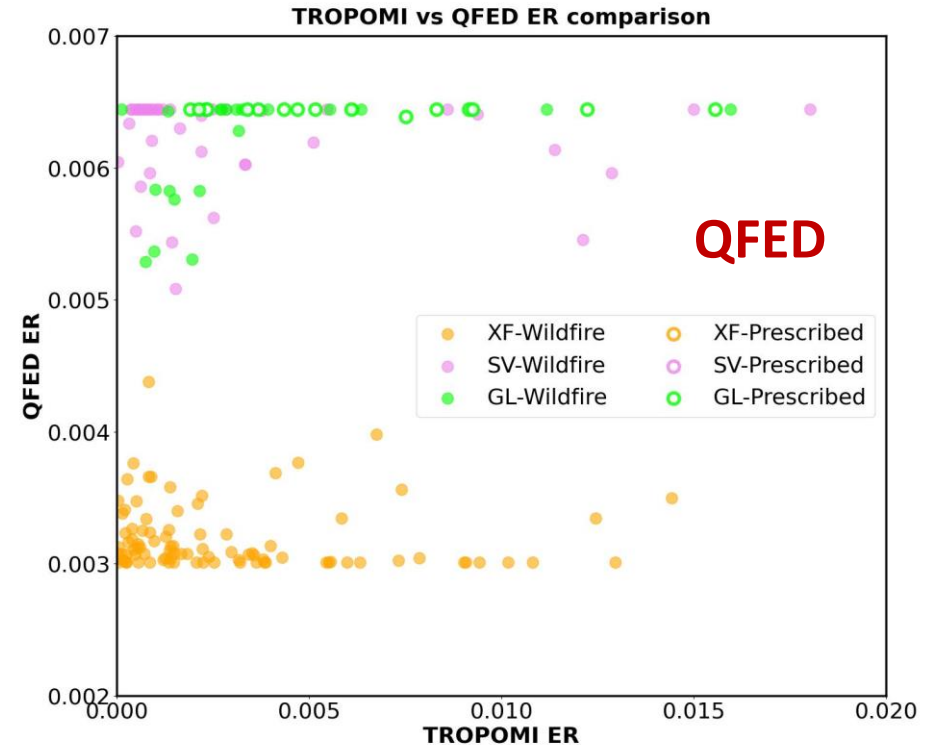
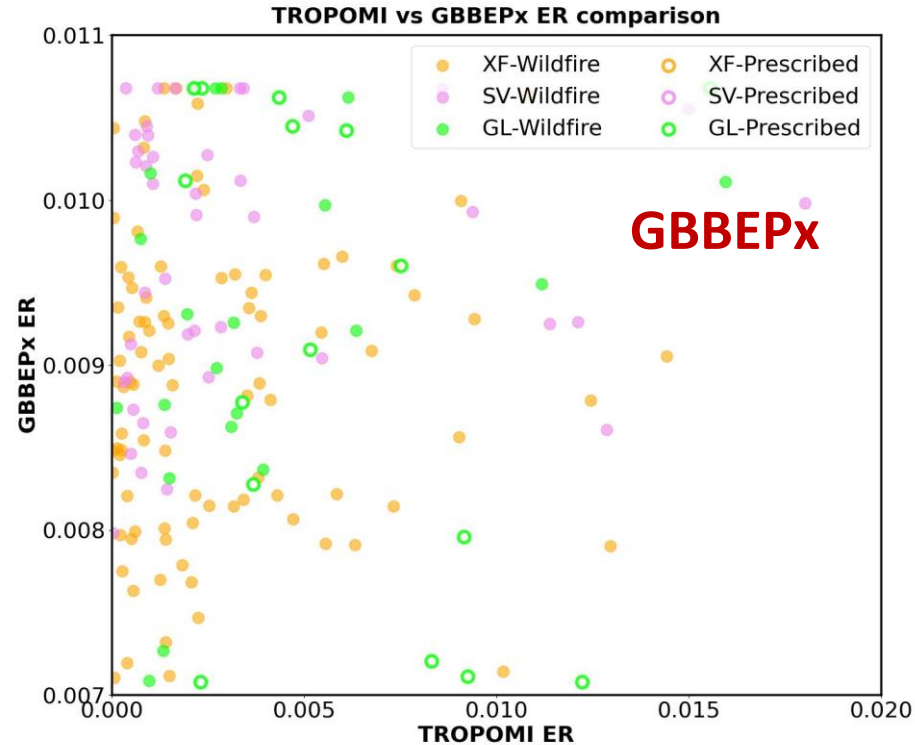
- Four land types identified in QFED, tropical forest (TF), extratropical forest (XF), savanna (SV), and grassland (GL), are analyzed. Note that there is no TF identified over CONUS.
- XF shows **higher  $E_{CO}$**  and **lower  $E_{NO_2}$**  while GL shows the **lowest  $E_{CO}$**  and the **highest  $E_{NO_2}$** , which is consistent with the emission factors used in emission inventories and reported in previous studies.
- Therefore, the high ER for XF and low ER for GL indicate the **capability of ER of identifying different land types**.
- However, the land type categorization in QFED does not consider fire types.

	XF	SV	GL
$E_{CO}$ ( $\text{mmol m}^{-2} \text{s}^{-1}$ )	0.011±0.017 (0.004)	0.006±0.008 (0.003)	0.004±0.005 (0.002)
$E_{NO_2}$ ( $10^{-3} \text{mmol m}^{-2} \text{s}^{-1}$ )	0.005±0.004 (0.003)	0.005±0.005 (0.003)	0.010±0.010 (0.005)
ER	0.002±0.003 (0.001)	0.012±0.054 (0.002)	0.019±0.079 (0.006)

Value: avg±std (med)

# ER's capability of distinguishing fire and land types

Note that fire and land types are identified based on EPA NEI and QFED, respectively.  
GBBEPx used the same land type identification as QFED.



- Most of XF and SV fires are identified as wildfires with ER lower than 0.005.
- Overall, ERs of GL fires are higher for prescribed fires and lower for wildfires, and show larger variation compared to XF and SV fires
- TROPOMI ER is sensitive more to fire types than land types.

# Source of uncertainties

- Selection of the **hyperparameters** used in emission estimation could be one of the key sources. For instance, the **diameter of fire center (L)** is given by assuming the identified fire grid is the fire center. However, based on the average fire size in 2000 – 2021 reported by National Interagency Fire Center (NIFC), the average diameter of fires is around 360 m which is far smaller than 0.1 degree.
- **Column-averaging winds** are assumed to be consistent during the day and the **location of fire plumes** in terms of height is not considered in emission estimation. These may introduce uncertainties in upwind box selection.
- Since CO has a relatively long lifetime, **CO emissions transported from far upwind** may contribute to the CO total-column measurement near fire sources, corresponding to the large impact of the transport term in emission estimation with a mean difference of -96%.

# Source of uncertainties: TROPOMI NO<sub>2</sub>

- For  $E_{\text{NO}_2}$ , the most important source of uncertainties would be **TROPOMI measurements**, since removing the annual medians introduces the largest impact in emission estimation with a mean difference over 300%.
- As emission estimation is based on the **differences between fire region and the background**, overestimation of the background and underestimation of peak values (Ialongo et al., 2020) could lead to the **underestimation of  $E_{\text{NO}_2}$** . Also, the high background level during summer and spatial homogenous NO<sub>2</sub> measurements during daytime (Goldberg et al., 2021) could make the differences between fire region and the background less significant.
- However, the good correlation between TROPOMI NO<sub>2</sub> with ground-based observations indicates TROPOMI's capability of capturing the day-to-day variability of NO<sub>2</sub> (Ialongo et al., 2020) and further **preproducing the seasonal variation of fire activities**.

# Conclusions

- TROPOMI emissions are overall **lower than fire emission inventories**.
- TROPOMI  $E_{CO}$  **shows a similar seasonal variation** to emission inventories with significant increases during summer, while  $E_{NO_2}$  **shows an opposite trend**.
- Because emission inventories estimate fire emissions based on prescribed emission factors, **inventory ERs fall in specific ranges** and are relatively consistent compared to TROPOMI.
- TROPOMI ER is lower for wildfires (extratropical forest fires) and higher for prescribed fires (grassland burnings), showing **the capability of distinguishing fire seasons associated with different fire types**.
- Most of XF and SV fires are identified as wildfires with ER lower than 0.005. Overall, GL fires show higher ER for prescribed fires and lower for wildfires.
- Except for land type, **fire type** is also an important factor determining fire emissions. Also, TROPOMI ER could be a useful input and improve the understanding of fire characteristics in fire activity models.

# References

- Burkholder, J. B.; Sander, S. P.; Abbatt, J. P. D.; Barker, J. R.; Huie, R. E.; Kolb, C. E.; Kurylo, M. J.; Orkin, V. L.; Wilmouth, D. M.; Wine, P. H. JPL Publication 15-10 Chemical Kinetics and Photochemical Data for Use in Atmospheric Studies, 18. NASA Jet Propulsion Laboratory, 2015, [https://jpldataeval.jpl.nasa.gov/pdf/JPL\\_Publication\\_15-10.pdf](https://jpldataeval.jpl.nasa.gov/pdf/JPL_Publication_15-10.pdf).
- Goldberg, D. L.; Anenberg, S. C.; Kerr, G. H.; Moheg, A.; Lu, Z.; Streets, D. G. TROPOMI NO<sub>2</sub> in the United States: A detailed look at the annual averages, weekly cycles, effects of temperature, and correlation with surface NO<sub>2</sub> concentrations. *Earth's Future*, 2021, 9, e2020EF001665, doi: 10.1029/2020EF001665.
- Ialongo, I.; Virta, H.; Eskes, H.; Hovila, J.; Douros, J. Comparison of TROPOMI/Sentinel-5 Precursor NO<sub>2</sub> observations with ground-based measurements in Helsinki. *Atmos. Meas. Tech.*, 2020, 13, 205–218, doi: 10.5194/amt-13-205-2020, 2020.
- Jaffe, D. A.; O'Neill, S. M.; Larkin, N. K.; Holder, A. L.; Peterson, D. L.; Halofsky, J. E.; Rappold, A. G. Wildfire and prescribed burning impacts on air quality in the United States. *J. Air Waste Manag. Assoc.*, 2020, 70:6, 583-615, doi: 10.1080/10962247.2020.1749731.
- Lama, S.; Houweling, S.; Boersma, K. F.; Eskes, H.; Aben, I.; Denier van der Gon, H. A. C.; Krol, M. C.; Dolman, H.; Borsdorff, T.; Lorente, A. Quantifying burning efficiency in megacities using the NO<sub>2</sub>/CO ratio from the Tropospheric Monitoring Instrument (TROPOMI). *Atmos. Chem. Phys.*, 2020, 20, 10295–10310, doi: 10.5194/acp-20-10295-2020.
- Lobert, J. M.; Warnatz, J. Emissions From the Combustion Process in Vegetation. In *Fire in the Environment: The Ecological, Climatic, and Atmospheric Chemical Importance of Vegetation Fires*; Crutzen, P.J., Goldammer, J.G., Eds, John Wiley & Sons Ltd. Chichester, 1993, 15-37.
- van der Velde, I. R.; van der Werf, G. R.; Houweling, S.; Eskes, H. J.; Veefkind, J. P.; Borsdorff, T.; Aben, I. Biomass burning combustion efficiency observed from space using measurements of CO and NO<sub>2</sub> by the Tropospheric Monitoring Instrument (TROPOMI). *Atmos. Chem. Phys.*, 2021, 21, 597–616, doi: 10.5194/acp-21-597-2021.
- Yokelson, Robert J.; Griffith, David W. T.; Ward, Darold E. Open-Path Fourier Transform Infrared Studies of Large-Scale Laboratory Biomass Fires. *Chemistry and Biochemistry Faculty Publications*, 1996, 44.

# Acknowledgements

- We acknowledge the followings for providing valuable datasets used in this study:
  - US EPA for the preliminary 2020 National Emissions Inventory (NEI).
  - European Space Agency (ESA) and National Aeronautics and Space Administration (NASA) Goddard Earth Sciences Data and Information Services Center (GES DISC) for TROPOMI.
  - National Oceanic and Atmospheric Administration (NOAA)/National Environmental Satellite Data and Information Service (NESDIS)/Office of Satellite and Product Operations (OSPO) for GBBEPx.
  - Atmospheric Chemistry Observations and Modeling (ACOM) in the National Center for Atmospheric Research (NCAR) for FINN.
  - European Centre for Medium-Range Weather Forecasts (ECMWF) for GFAS.
  - Global Modeling and Assimilation Office (GAMO) of NASA for QFED.
  - NOAA/Earth System Research Laboratories (ESRL)/Global Systems Laboratory (GSL) and the Center for High Performance Computing (CHPC) at the University of Utah for HRRR.

Backup slides



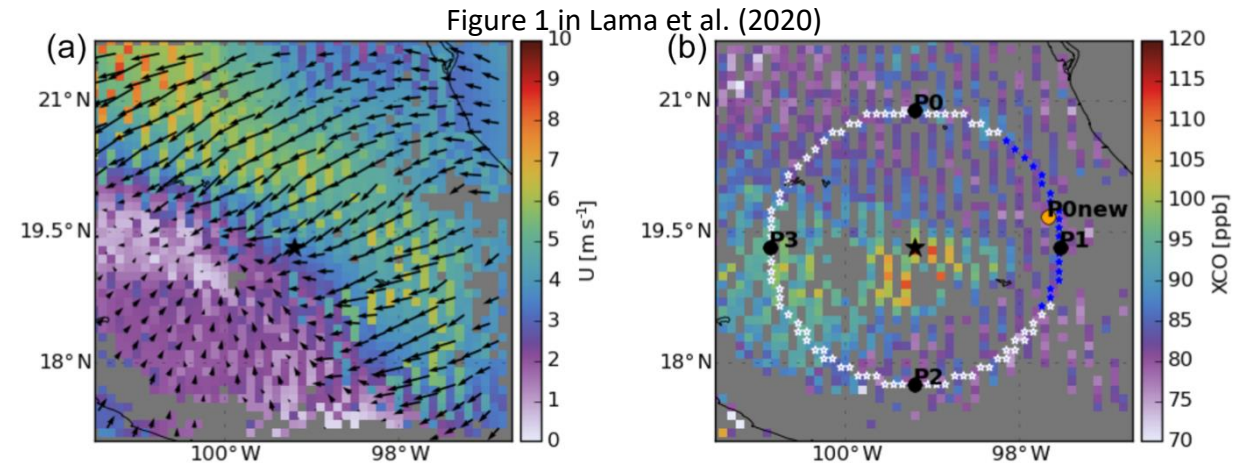
# ER calculation:

## Local sampling method (Van der Velde et al. 2021)

- Compare the combustion coefficients for fire regions.
- Convert TROPOMI observations into 0.1 x 0.1 degree resolution.
- **Data selection:**
  - CO: quality flag > 0.7
  - NO<sub>2</sub>: quality flag > 0.75 and cloud fraction < 0.5
  - Measurements over snow- and ice-covered surfaces are removed.
- A 10 x 10 degree fire box with fire point as the center and a 5 x 5 degree upwind box are selected. Location of the upwind box is determined based on **virtual inspection**.
- For each fire point, fire-affected and background column densities are defined as the **averages of the fire box and upwind box**, respectively.
- ER is calculated as the ratio of **the enhancements of total-column NO<sub>2</sub> and CO** associated with fires ( $ER = \Delta X_{NO_2} / \Delta X_{CO}$ ). Enhancement is defined as the differences between fire-affected and background column densities.

# ER calculation: Upwind background (Lama et al. 2020)

- Compare the combustion coefficients for megacities.
- Convert TROPOMI observations into 0.1 x 0.1 degree resolution.
- **Data selection:**
  - CO: quality flag > 0.7
  - NO<sub>2</sub>: quality flag > 0.75
- City-core region and upwind area surrounding the megacities are selected. The upwind area is determined based on given skirt radius and column-average winds below 200 m.
- For each fire point, city-affected and background column densities are defined as the averages of the city-core and upwind area, respectively. The difference between two are defined as the enhancement of total-column NO<sub>2</sub> and CO ( $\Delta XNO_2$  and  $\Delta XCO$ ).



# ER calculation: Upwind background (Lama et al. 2020)

- To compare TROPOMI with emission inventories, a relationship between the inventory emission ratio ( $E_{\text{NO}_2}/E_{\text{CO}}$ ) and the ratio of TROPOMI column enhancement ( $\Delta\text{XNO}_2/\Delta\text{XCO}$ ) is formulated by taking the combined effect of **atmospheric transport**, **chemical loss**, and the **averaging kernel** into account.

$$E_{\text{CO}} = \frac{U}{l_x} \Delta\text{XCO}$$

$$E_{\text{NO}_2} = \Delta\text{XNO}_2 \left( \frac{U}{l_x} + \frac{1}{\frac{1}{K[\text{OH}]}} \right)$$

$$\frac{E_{\text{NO}_2}}{E_{\text{CO}}} = \frac{\Delta\text{XNO}_2}{\Delta\text{XCO}} \frac{\left( \frac{U}{l_x} + K[\text{OH}] \right)}{\frac{U}{l_x}} \frac{1}{(1 - A_{\text{influence}})}$$

A1-A3 in Lama et al. (2020)

- U: WS in 200m a.g.l. ( $\text{ms}^{-1}$ )
- $l_x$ : diameter of the city center (m)
- K: NO<sub>2</sub>-OH reaction rate,  $2.8 \times 10^{-11} \times (T/300)^{-1.3} \text{ cm}^3 \text{ mole}^{-1} \text{ s}^{-1}$  (Burkholder et al., 2015). T (K) and OH ( $\text{mole cm}^{-3}$ ) are the boundary layer average temperature and OH concentration.
- $A_{\text{influence}}$ : the influence of the averaging kernel on  $\Delta\text{XNO}_2 / \Delta\text{XCO}$  (~9-10%)